**Integrated Systems and Technologies:** *Mathematical Oncology*

Cancer Research

# Cancer Stem Cell Tumor Model Reveals Invasive Morphology and Increased Phenotypical Heterogeneity

Andrea Sottoriva[1], Joost J.C. Verhoeff[2], Tijana Borovski[2], Shannon K. McWeeney[3,4], Lev Naumov[1], Jan Paul Medema[2], Peter M.A. Sloot[1], and Louis Vermeulen[2]

## Abstract

The recently developed concept of cancer stem cells (CSC) sheds new light on various aspects of tumor growth and progression. Here, we present a mathematical model of malignancies to investigate how a hierarchical organized cancer cell population affects the fundamental properties of solid malignancies. We establish that tumors modeled in a CSC context more faithfully resemble human malignancies and show invasive behavior, whereas tumors without a CSC hierarchy do not. These findings are corroborated by *in vitro* studies. In addition, we provide evidence that the CSC model is accompanied by highly altered evolutionary dynamics compared with the ones predicted to exist in a stochastic, nonhierarchical tumor model. Our main findings indicate that the CSC model allows for significantly higher tumor heterogeneity, which may affect therapy resistance. Moreover, we show that therapy which fails to target the CSC population is not only unsuccessful in curing the patient, but also promotes malignant features in the recurring tumor. These include rapid expansion, increased invasion, and enhanced heterogeneity. *Cancer Res; 70(1); 46–56. ©2010 AACR.*

## Introduction

Malignancies arise after sequential accumulations of mutations in oncogenes and tumor suppressor genes (1). During the process of malignant transition, fundamental regulatory mechanisms are lost. The cancerous cell population has unlimited growth potential, evades the immune system and apoptosis, and often acquires the ability to breach tissue boundaries and expand into foreign environments (1). The cancer stem cell (CSC) concept sheds new light on all of these features (2, 3). In this study, we investigate the influence of a hierarchical organization of malignant clones on tumor growth, evolution, invasion, and morphology using a multi-scale cellular automaton–based computer model (4).

***CSCs.*** Malignancies are highly heterogeneous tissues containing largely diverse cancer cell populations as well as other cells such as fibroblasts and macrophages (1). The dominant genetic view of malignancies explains the heterogeneity in cancer cells with the presence of genetically diverse clones emerging from the continuous acquiring of additional genetic lesions by cancer cells. Such clones compete for resources, resulting in a highly dynamic process known as Tumor Darwinism (5). In this article, we refer to this view of malignancies as the classical model. Although this model greatly contributes to our understanding of malignancies, recent experimental evidence suggests an additional layer of complexity. The heterogeneity present in tumors could, in part, be the result of the diversity in differentiation grade of genetically identical cells (3, 6). For example, in glioblastoma multiforme, cells with an immature phenotype expressing the cell surface marker AC133 are the cells that fuel tumor growth and have the exclusive capacities to self-renew, differentiate, and transplant the malignancy into severe combined immunodeficiency mice (7). Self-renewal and spin-off of differentiated cells are features shared with normal stem cells, and therefore, cells with such features in malignancies are defined as CSCs (6, 8).

### Major Findings

This research shows that the hierarchical organization of malignant clones, as advocated in the CSC concept, has major implications for tumor biology. CSC-driven tumor growth intrinsically orchestrates tumor invasion, influences clonal selection, and has crucial consequences for the development of successful cancer treatments.

**Authors' Affiliations:** [1]Computational Science, Faculty of Science, University of Amsterdam and [2]Laboratory for Experimental Oncology and Radiobiology (LEXOR), Center for Experimental Molecular Medicine, Academical Medical Center, Amsterdam, the Netherlands; [3]Division of Biostatistics, Department of Public Health and Preventive Medicine, Oregon Health and Science University, and [4]OHSU Knight Cancer Institute Portland, Portland, Oregon

**Note:** Supplementary data for this article are available at Cancer Research Online (http://cancerres.aacrjournals.org/).

Current address for A. Sottoriva: Department of Oncology, University of Cambridge, CRUK Cambridge Research Institute, Li Ka Shing Centre, Cambridge, UK.

P.M.A. Sloot and L. Vermeulen share senior authorship.

**Corresponding Author:** Louis Vermeulen, Academic Medical Center, Meibergdreef 9, 1105AZ, Amsterdam, the Netherlands. Phone: 31-20566-4777; Fax: 31-20697-7192; E-mail: l.vermeulen@amc.uva.nl.

**doi:** 10.1158/0008-5472.CAN-09-3663

## Quick Guide to Equations and Assumptions

### Proliferation

The stem cellular automaton (SCA) model is a hybrid cellular automaton (4) in which a biological cell is a point (10 × 10 μm) in a lattice. Each point can be a normal cell, a cancer cell, or a necrotic cell, and has the attributes in Table 1. After a cell division, an empty place is created by shifting the surrounding cells outward.

**Major Assumptions.** Proliferation concentrates in the proximity of the tumor borders where oxygen levels are higher, the pH is more normal, and the pressure is lower (12–14). To model this, we assume the probability of a cell to divide to be linear, from 1 at the tumor edges to 0 at a distance $\lambda$ = 600 μm (60 cells) from the tumor margins.

### Metabolism

$$\frac{\partial c}{\partial t} = D_c \nabla^2 c - \kappa n \qquad \text{(A)}$$

Oxygen is critical for cell survival, it diffuses into the tumor and it is consumed by cancer cells. Upon discretization of Eq. (A), cancer cells $n$ consume oxygen at rate $\kappa$.

**Major Assumptions.** Oxygen around the tumor is kept constant by the vascular system. Cell quiescence occurs below an oxygen threshold $\kappa^s$ and necrosis below an oxygen threshold $\theta$.

### Migration

$$\frac{\partial c}{\partial t} = D_n \nabla^2 n \qquad \text{(B)}$$

During tumor progression, cancer cells lose cell-to-cell attachment and invade the surrounding tissues (15). This process is modeled using the Hybrid Discrete-Continuum Technique (16), in which cancer cells $n$ disperse with coefficient $D_n$. To simulate adhesion, we allow cell movement if the number of neighboring tumor cells $g \geq \alpha$, where $\alpha$ is the adhesion coefficient of the cell in the range 0 to 4.

**Major Assumptions.** Cells move according to a random motion coefficient $D^n$ and an adhesion coefficient $\alpha$.

### CSCs

CSCs divide symmetrically with probability $P_S$ and asymmetrically with probability $1 - P_S$. Two new CSCs result from the former, a differentiated cancer cell (DCC) and a CSC from the latter. CSCs possess unlimited replicative potential and self-renewal whereas DCCs can divide up to $H$ times. A CSC growth model has small $P_S$ values, whereas for $P_S = 1$, we simulate the classical model of malignancies.

**Major Assumptions.** We fix $H = 5$ and vary $P^S$ to simulate different CSC frequencies. As suggested experimentally for both CSCs and normal stem cells, we have restricted migration to CSCs (17–20).

### Tumor Evolution

We introduced tumor phenotypical heterogeneity in some experiments by assuming that every CSC self-renewal division has a chance $P_{Mut}$ for the new CSC to acquire a different phenotype (see Supplementary Materials and Methods).

**Major Assumptions.** Only CSCs contribute to tumor evolution in the long run.

***Modeling tumor growth.*** Tumor growth is generally accepted to be the result of several highly complex interacting processes. Fundamental cellular characteristics such as genetic and epigenetic features influence signal transduction route activities that in turn control cellular functions such as mitosis, apoptosis, and cell migration. In addition, environmental factors including nutrients and growth factor concentrations interplay with these processes. To study the emergent properties of such systems regarding proliferation speed, infiltrative growth, and phenotypical evolution of cancer, advanced mathematical models have been developed (9–11). Here, we apply computational modeling techniques to investigate the consequences of hierarchically organized cancer cell populations on solid tumor growth dynamics and progression. We describe

**Table 1.** Cellular and microenvironmental variables in the SCA model

| Variables | Symbol | Value | Reference/justification |
|---|---|---|---|
| Proliferation speed (average cell cycle duration) | $T$ | 20 h | (44) |
| $O_2$ diffusion coefficient | $D_c$ | $10^{-5}$ cm$^{-2}$ s$^{-1}$ | (16) |
| $O_2$ concentration, healthy tissue | $\omega$ | $10^{-4}$ g cm$^{-3}$ | (16, 45) |
| $O_2$ consumption, proliferative cells | $\kappa_p$ | $10^{-6}$ g cm$^{-3}$ s$^{-1}$ | (46) |
| $O_2$ consumption, senescent cells | $\kappa_s$ | $5 \times 10^{-7}$ g cm$^{-3}$ s$^{-1}$ | (47) |
| $O_2$ concentration resulting in necrosis | $\theta$ | $5 \times 10^{-7}$ g cm$^{-3}$ s$^{-1}$ | Senescent consumption as minimum concentration for cell survival |
| Random mobility | $D_n$ | $10^{-10}$ cm$^{-2}$ s$^{-1}$ | (48) |
| Maximum number of generations generated by DCCs | $H$ | 5 | We choose to fix $H$ to 5 and vary $P_S$ to generate various CSC fractions (3) |

NOTE: Variables used in the SCA model. See the Quick Guide and Materials and Methods for details.

that implementing the developing concept of CSCs in a mathematical tumor growth model directly results in an invasive morphology. Moreover, we found that hierarchical organized malignant clones have highly altered evolutionary dynamics. Most strikingly, the CSC organization promotes phenotypical heterogeneity, a feature that could have immediate consequences for therapy resistance.

## Materials and Methods

***SCA model.*** We developed a hybrid tumor growth model based on cellular automata (4) and partial differential equations. We refer to this model as the SCA model. In the SCA model, the individual cancer cell is the fundamental unit of the tumor, we simulate its proliferation, metabolism, migration, stemness, and differentiation (see Quick Guide and Supplementary Materials and Methods).

Implementing the CSC model of malignancies means to simulate cancer cells with different replicative potential within the tumor. For simplicity, we assume that in our model there are only two types of cells: CSCs and DCCs. CSCs possess unlimited replicative potential and could either generate new CSCs (with a probability $P_S$) or DCCs. DCCs can divide for a maximum of $H$ generations before stopping to proliferate irreversibly. This method yields a hierarchy with CSCs at the top and DCCs at the bottom. We simulate the classical model of malignancies, in which all cells possess tumor growth–promoting capacities, by simply setting $P_S = 1$. In such a situation, all cells possess stem cell characteristics. Using this method, we have an intuitive way to compare the flat, classical tumor model with the hierarchically organized CSC model.

## Results

***Emergent invasive morphology.*** Computational modeling allows the exploration of highly complex systems, such as tumor growth. In this study, we have used a computational tumor growth model to test the consequences of hierarchical organized clones on a vast range of areas of tumor biology. These include tumor growth dynamics and morphology, but also tumor evolution and therapeutic effects. The applied computational modeling technique allows us to get more insight into the underlying dynamics of these aspects of cancer growth and progression that would be impossible in a conventional experimental biological setting.

First, we investigated how tumor growth dynamics are altered upon varying the CSC fraction. In the SCA model, this corresponds to changing the variable $P_S$. For high values of $P_S$, we expect to model the classical interpretation of tumors because all cell divisions are symmetrical and all cells are therefore clonogenic. In contrast, low values of $P_S$ represent the CSC model. We simulated the growth of tumors with $P_S = 1$, $P_S = 0.1$, and $P_S = 0.03$ with the variables described in Table 1.

Figure 1*A* shows the fraction of CSCs on the total amount of tumor cells for different values of $P_S$. The selected $P_S$ values correspond to CSCs populations comprising roughly 100%, 1%, or 0.1% of the total tumor volume and therefore cover mainly the CSC fractions observed in a variety of solid malignancies (2). In the CSC model ($P_S = 0.1$ and $P_S = 0.03$), small (early) lesions have relatively high fractions of CSCs, although this number decreases and tends to stabilize when the tumor progresses. This observation is supported by *in vivo* studies that find increased numbers of CSC marker–bearing cells in micrometastases compared with larger tumors (21). This indicates that even with fixed self-renewal rates ($P_S$), this phenomenon is intrinsic to lesions initiated by a single CSC although environmental factors influencing self-renewal frequencies are also likely to contribute. Tumor growth curves for various $P_S$ values all display the classical Gompertzian-like growth kinetics. However, as expected with equal cell cycle durations, the self-renewal rates of the stem cell fraction influences proliferation rate greatly, hence, low self-renewal rates (small $P_S$) correspond to slow tumor growth (Fig. 1*B*). Interestingly, the decrease in accumulation of tumor volume is accompanied by a stabilization of the fraction of CSCs, suggesting an intimate relationship between these two processes.

Spatially, all experiments display a three-layered structure consisting of an external proliferative area, an inner senescent layer, and a necrotic core. However, tumor morphologies for different $P_S$ values are remarkably dissimilar

(Fig. 1*D*). For $P_S$ = 1, in which there is no hierarchy, a symmetrical, sphere-like tumor morphology is generated that closely resembles early tumor growth models (22, 23). In contrast, the shape of the tumors generated with low $P_S$ values is highly irregular (especially $P_S$ = 0.03). CSC-driven tumors yield highly invasive morphologies with fingering fronts and clusters of cancer cells beyond the tumor margin, driven by the mobility and the exclusive proliferative properties of CSCs (Movies S1 and S2).

From Fig. 1*C*, it is evident how hierarchically organized tumors ($P_S$ = 0.03 and $P_S$ = 0.1) generate a higher degree of invasiveness (see Supplementary Materials and Methods), compared with tumors in the classical model ($P_S$ = 1). It is important to note that the intrinsic properties of the cells in the classical tumor and the stem cells in the CSC-driven tumor are completely identical.

Magnification of a tumor border in a CSC-fueled tumor growth model ($P_S$ = 0.03) shows how CSCs migrate beyond the margins of the tumor mass. CSCs colonize the surrounding tissue and expand locally, forming small satellites that grow back into, and are engulfed by, the main tumor mass (Fig. 2*A*). This is accompanied by the observation that

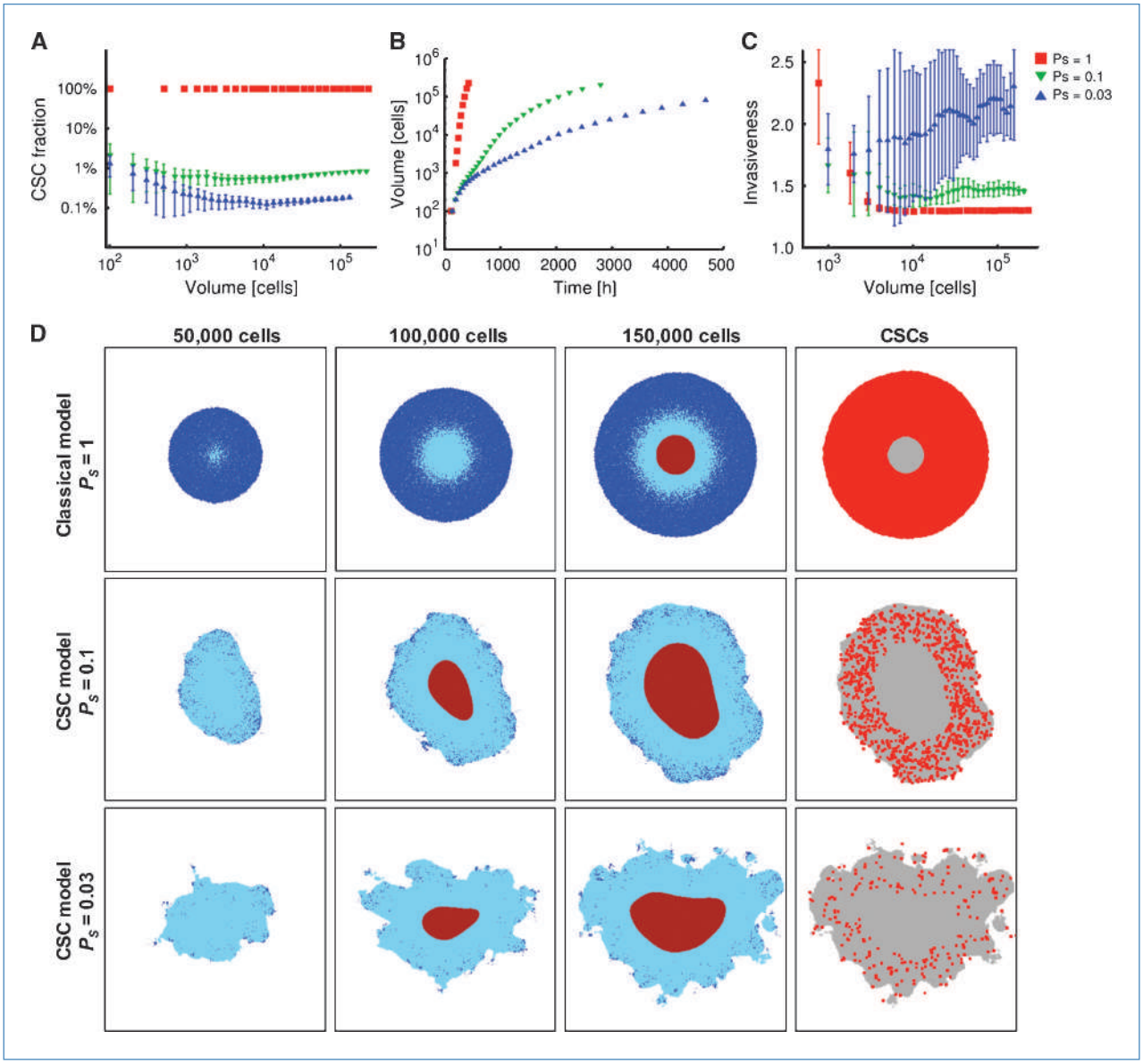


**Figure 1.** Emergent invasive behavior in the CSC model. *A,* different $P_S$ values result in different CSC fractions. *B,* growth curves for different $P_S$ values. *C,* quantitative measure for invasiveness shows increasing invasive behavior with declining $P_S$. *A* to *C, bars,* SD ($n$ = 16). *D,* hierarchical organization in the SCA model affects tumor morphology. Tumors for different values of self-renewal probability ($P_S$) and different volumes. *Dark blue,* cells which have divided within the last 48 h (depicted larger); *light blue,* nondividing cells; *brown,* necrotic center. *Right,* localization of CSCs in the tumor mass. *Gray,* tumor mass; *red,* CSCs (depicted larger). In all figures, 6 × 6 mm of tissue are represented. See also Movies S1 and S2.

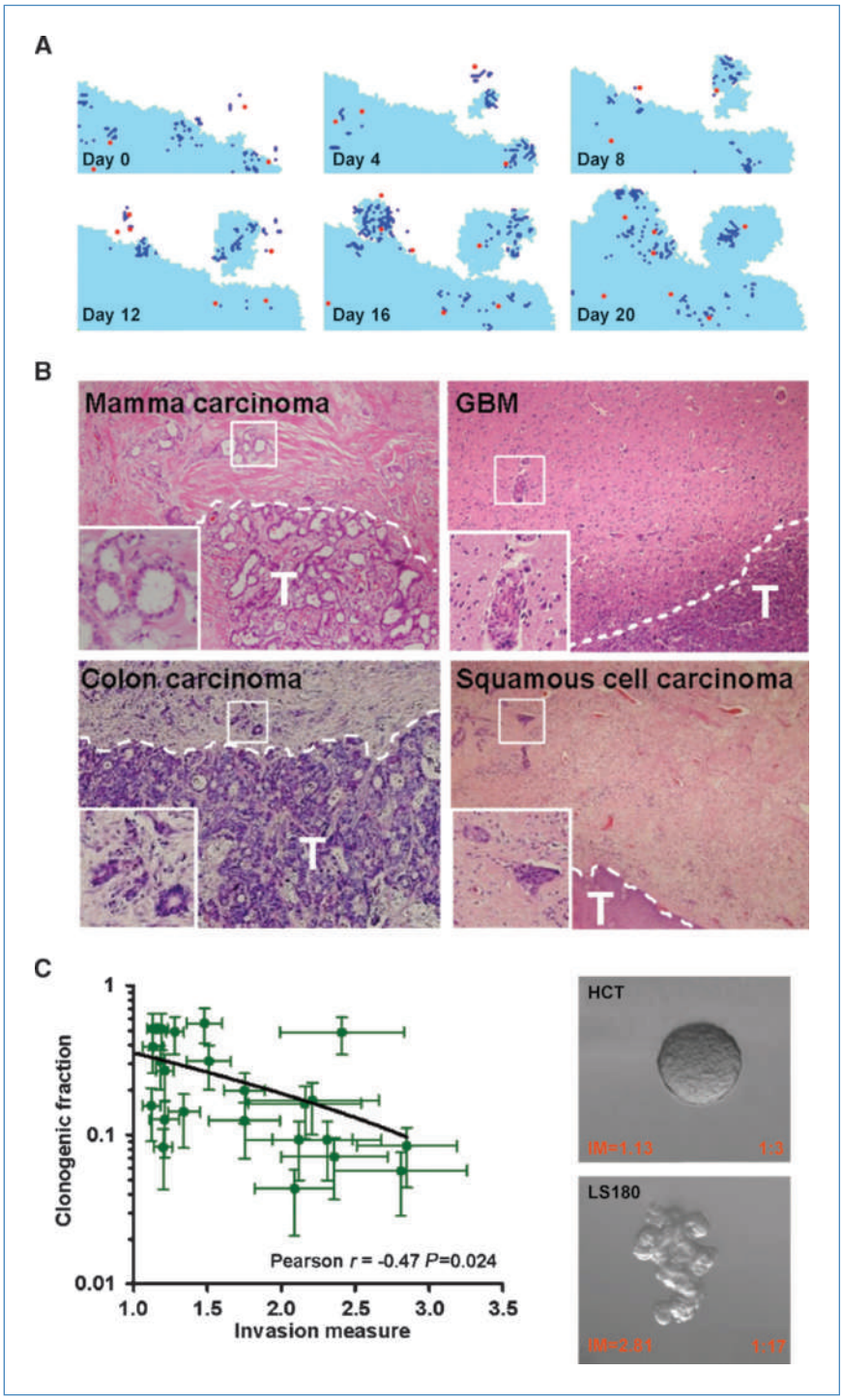


**Figure 2.** Invasive behavior *in silico, in vivo*, and *in vitro. A,* close-up of tumor border showing invasive behavior for $P_S = 0.03$. CSCs (*red*) infiltrate surrounding tissue and spin-off DCCs that proliferate (*dark blue*). Small satellites are formed in the surrounding normal tissue (*white*) and grow back to and are engulfed by the main tumor mass. Nondividing cells (*light blue*). *B,* representative figures of various malignancies. All images reveal island-like formations at the rim of the main tumor mass (*T*). These findings are in line with tumor expansion as predicted by the SCA model that implements a CSC hierarchy. *C,* cell lines ($n = 24$) have been plated at clonal density in Matrigel. Simultaneously, the clonogenic fraction of the lines has been determined by limiting dilution analysis. A significant ($P = 0.02$) inverse relationship exists between clonogenicity and invasion as quantified by the measure of invasiveness we defined. Two examples of cell lines are shown and invasiveness (*IM*) and clonogenicity are indicated (*right*). See Supplementary Figs. S2 to S5 and Supplementary Table S1 for details.

the invasive behavior of individual experiments that make up Fig. 1*C* occurs in a wave-like fashion (Supplementary Fig. S1). These results are paralleled by recent findings in a different model system in which high migration levels in a small subset of cells give rise to small proliferating extratumoral lesions and therefore tumors are "conglomerates of self-metastasis" as the authors propose (24).

In an endeavor to validate these observations from our computational model, we investigated human tumor specimens. Close examination of the histology of different highly diverse human malignancies displayed a relatively confined large tumor mass with clearly detached tumor cells forming small lesions in the surrounding normal tissue (Fig. 2*B*). This exemplifies that human tumor histology contains indications

of a stepwise infiltration and colonization of the surrounding tissue as our model predicts would follow from a hierarchical organized malignancy. Next, we attempted to determine the relationship between CSC fraction and invasive properties, as predicted by the model, using *in vitro* cell culture (Fig. 2*C*; Supplementary Figs. S2–S5 and Table S1). We determined the clonogenicity of a set of various cell lines ($n$ = 24) as a surrogate for their CSC fraction. Additionally, we quantified the invasive properties of clonally derived structures with our measure of irregular morphology both on adherent plates and in Matrigel for all these lines. A significant inverse relationship between clonogenic fraction and the invasive properties of these lines exists. This implicates that tumor structures driven by a small fraction of clonogenic cells tend to generate a more irregular and invasive morphology, a finding that corroborates the predictions of our model. Combined, we take this as evidence that the SCA model based on the CSC concept closely resembles tumor growth patterns and morphology.

***Expansion of the model in three dimensions retains invasive morphology.*** To show that our results are not limited to two dimensions only, we expand the SCA model to three dimensions (see Supplementary Materials and Methods). The three-dimensional SCA model reproduces the invasive tumor morphology induced by the hierarchical organization, yielding three-dimensional fingering tumor fronts and clusters of cancer cells beyond the borders of the main tumor mass (Fig. 3*A*; Movie S3). On the contrary, again a classical model with equal volume does not display any apparent invasive pattern and instead exhibits a spherical morphology (Fig. 3*B*; Movie S4). We therefore propose that the CSC model, in contrast to the flat model, more faithfully reproduces the human tumor morphology for both the two-dimensional and the three-dimensional implementations.

***CSC organization stimulates tumor heterogeneity.*** The dominant model evoked to explain the advancement of malignancies is clonal evolution, as was first proposed by Nowell (5). The term effective population size is used in population genetics to indicate the fraction of total individuals in a population that effectively contributes to the next generation and are therefore evolutionarily relevant. Hence, the effective population size in a CSC-driven malignancy is smaller than in the classical model because only mutations in the CSC compartment contribute to the evolutionary process (2). To implement clonal evolution in our model, we assume that, at each symmetrical division a CSC has a probability $P_{\mathrm{Mut}}$ to acquire a genetic hit and generate a daughter cell with a different phenotype selected from a randomly

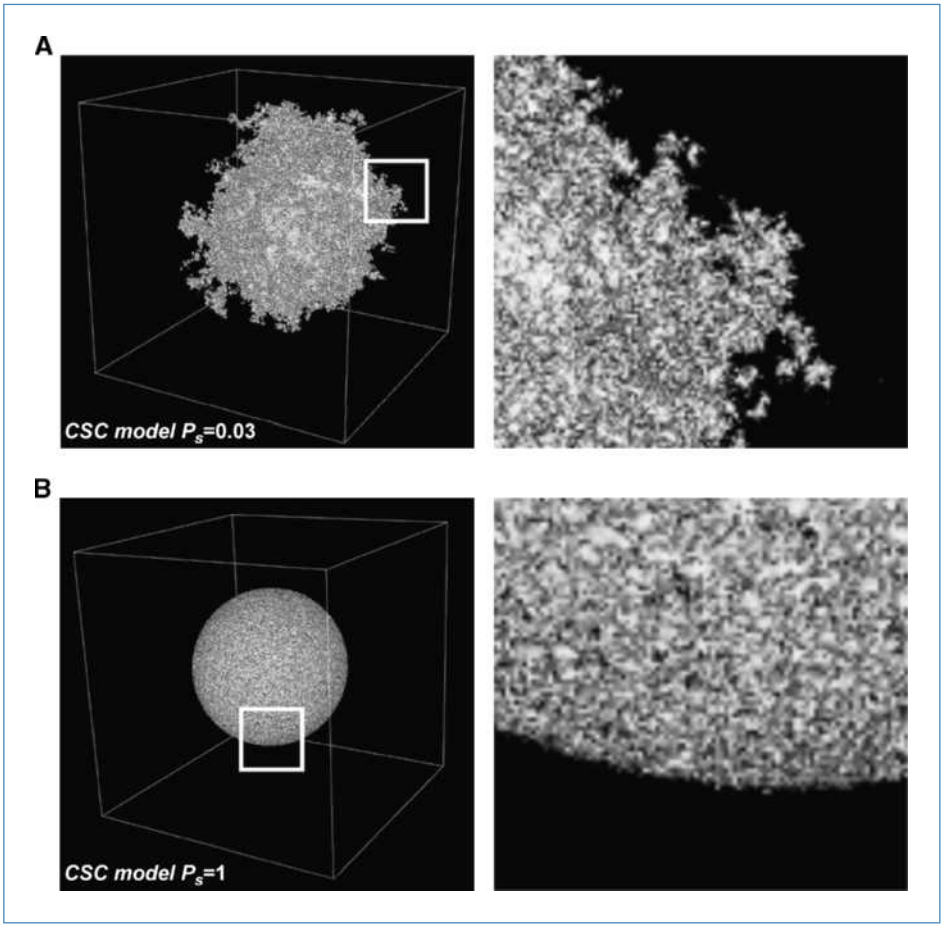


Figure 3. Expansion of the model in three-dimensions retains infiltrative morphology. Three-dimensional representation of CSC-driven tumor growth (*A*, $P_S$ = 0.03) and of the classical tumor model (*B*, $P_S$ = 1). *A* and *B*, $7 \times 10^6$ cells are represented. *Inset*, region that is enlarged in the right image. Normal tissue (*black*) and tumor cells (*white*). Cube represents $400^3$ cell lattice. See also Supplementary Movies S3 and S4.

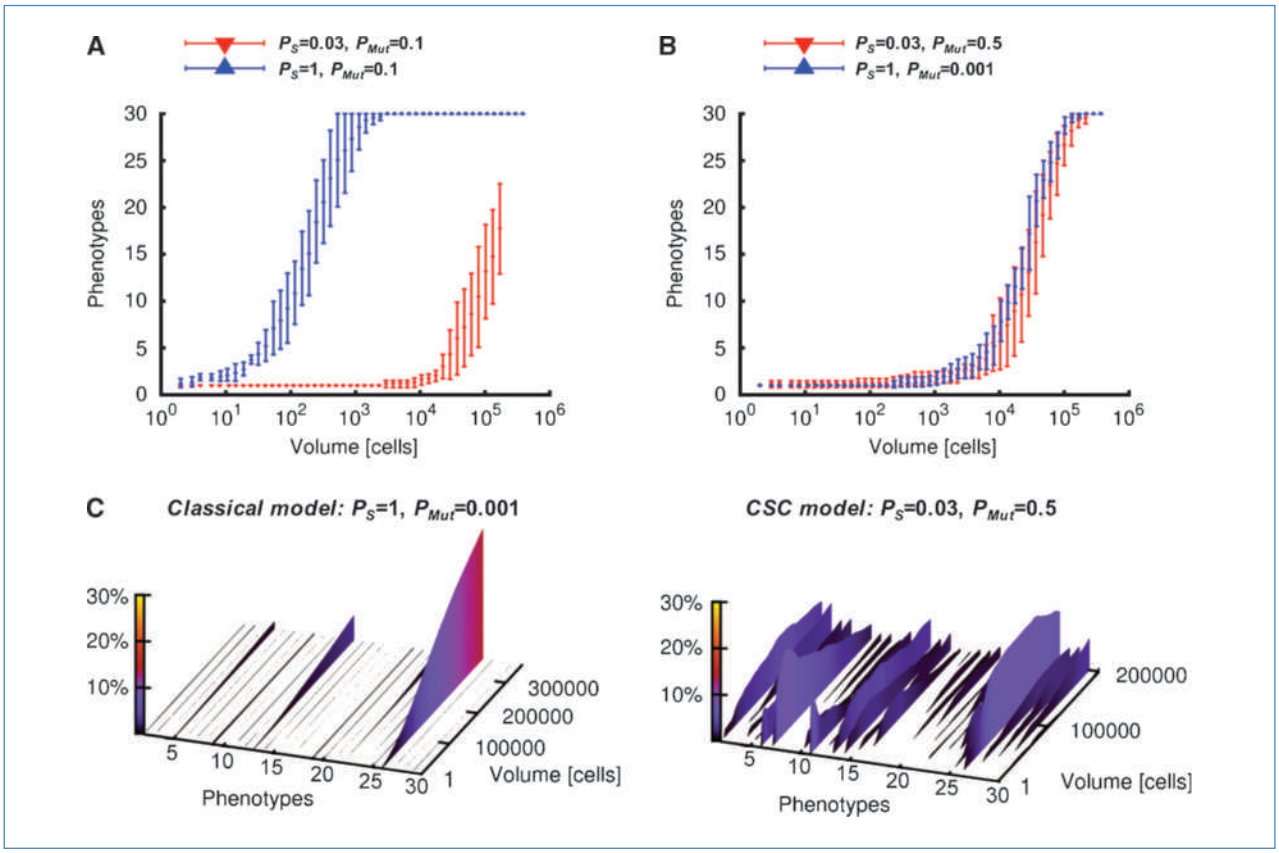


**Figure 4.** Tumor evolution and phenotypical selection in a cancer stem cell context. Phenotypes are randomly generated and possess traits listed in Supplementary Table S3. *A,* with equal mutation rates ($P_{Mut}$ = 0.1), the cumulative amount of phenotypes that emerge is higher in the classical model ($P_S$ = 1) compared with the CSC model ($P_S$ = 0.03). *B,* we adapted $P_{Mut}$ to obtain an equal rate of emergence of phenotypes. *C,* under equal conditions, the phenotypes in the CSC model are more diverse compared with the classical model. A representative example is shown, see also Supplementary Movies S5 and S6. *A* and *B, bars,* SD ($n$ = 8). *C,* fraction of cells for each newly generated phenotype. The original phenotype "1" is ignored. For an average of eight experiments, see Supplementary Figs. S6*B* and S6*C*.

generated pool of 30 phenotypes (Table S2 and S3; see Supplementary Materials and Methods). Under an equal mutation rate ($P_{Mut}$ = 0.1), the CSC model exhibits a slower acquisition of new phenotypes due to its smaller effective population size (Fig. 4*A*), but also shows a radically different selection process. Strikingly, although the rate of emergence of new phenotypes is much lower than observed in the classical model, a wide range of newly acquired phenotypes expands and contributes to the malignancy (Supplementary Fig. S6*A* and *B*).

To compare the phenotypical selection more closely, we synchronize the pace at which new traits emerge. Evolutionarily, a CSC model with $P_S$ = 0.03 and $P_{Mut}$ = 0.5 corresponds to a classical model with $P_S$ = 1 and $P_{Mut}$ = 0.001 (Fig. 4*B*). Intriguingly, despite this adaptation of the mutation pace, the two models differ substantially in the way they exercise clonal selection. From a representative example in Fig. 4*C*, it is evident that the CSC model allows for a much higher phenotypical heterogeneity whereas the classical model seems to select for a small number of aggressive clones (average result in Supplementary Fig. S6*C*). Quantification of the heterogeneity clearly underscores this (Supplementary Fig. S7*A* and Supplementary Materials and Methods). It is important to realize that the selective pressure from the environment is equal in both models. This, combined with the equal rate of new phenotype occurrence, suggests that the geometric properties of the CSC model promote heterogeneity. We argue that the intrinsic properties of the CSC model might propel an alternative process to natural selection, referred to as genetic drift (25). In populations with small effective population sizes, sampling errors are frequent and might allow for the expansion of clones with no clear survival benefit. Interestingly, the invasive properties of the CSC model might fuel such a sampling error promoting mechanism. The phenomenon we observe at the tumor margins during invasion: a CSC migrating out of the tumor initiating a small satellite lesion, resembles the Founder Effect (26). The Founder Effect occurs when a new population is established by a low number of individuals from a larger population, this process is often accompanied by a loss of phenotypical variation in the new population due to sampling errors. In such a scenario, the new generation can

differ substantially from the previous and is not in direct competition for nutrients and space. This implies that the pattern of tumor growth in the CSC model stimulates genetic drift at the infiltrative edges of the tumor and therefore promotes phenotypical heterogeneity.

***Dynamics of therapeutic interventions in hierarchical organized malignancies.*** After having established the effects of CSC-driven tumor growth on the invasion and evolution of malignancies, we now explore the crucial topic of therapeutic intervention and tumor relapse. CSCs have been suggested to be more resistant to therapeutic interventions such as chemotherapy or irradiation compared with their differentiated counterparts (27, 28). Also tumors that relapse after seemingly successful therapy are believed to regrow from the CSC that survived the therapeutic regimen (27). Here, we investigate the dynamics associated with therapeutic interventions that are either selective for non-CSCs or equally efficient against both cell types. We find that the morphology and growth kinetics of relapses for both types of therapeutic interventions are very much different (Fig. 5; see Supplementary Materials and Methods). Regrowth after therapy that specifically targets DCCs is accompanied by enhanced invasive growth patterns whereas relapsing tumors after stochastic tumor cell killing are similar to the malignancy before

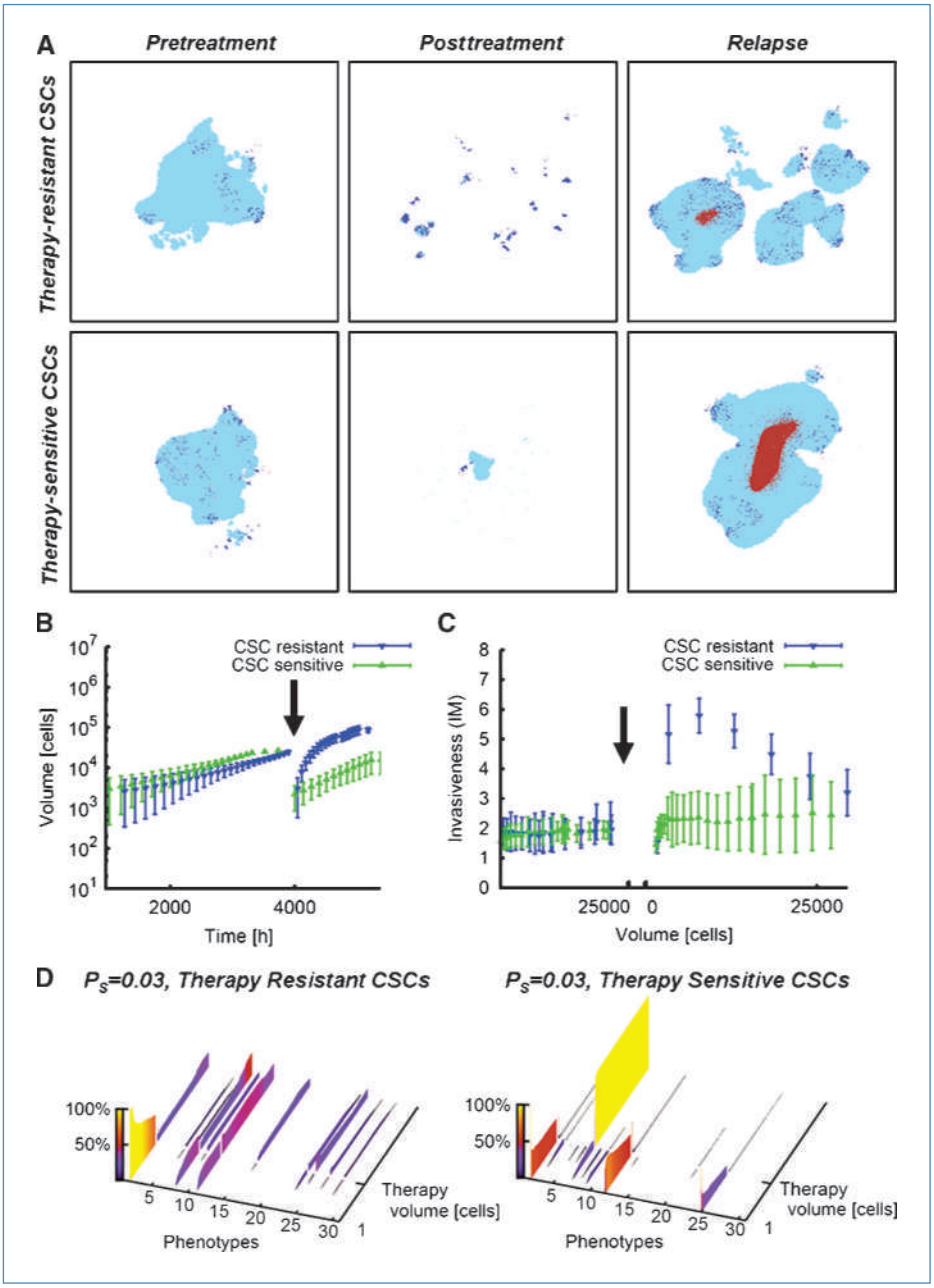


**Figure 5.** Dynamics of therapeutic intervention in hierarchical organized malignancies. *A,* effects of therapy in simulated tumors considering CSCs to be resistant to treatment (*top*) or sensitive to treatment (*bottom*). *Left,* pretreated tumor at $V_T$ = 25,000 cells. *Right,* after treatment and relapsed tumor for $V_{Relapse} = V_T$. *B,* growth curves of tumor relapse. Whereas therapy-sensitive CSCs recapitulate the initial growth pace, resistant CSCs yield a faster growth at relapse. *C,* a marked increase of invasive morphology just after treatment occurs particularly in the case of resistant CSCs. *B* and *C, arrows,* therapy ($n$ = 8). *D,* phenotype distribution in the two cases of therapy response assuming no further mutation to occur after therapy (see Supplementary Fig. S8 for an average of eight experiments). Although a treatment-resistant CSC-driven tumor is able to recapitulate the clonal features of the initial malignancy by conserving the initially developed heterogeneity, for therapy-sensitive CSCs, the recurrent tumor is highly altered in terms of phenotypes.

treatment (Fig. 5*A*). Simultaneously, in case CSCs are resistant to therapy, the pace at which the malignancy relapses is greatly enhanced due to the relatively high fraction of CSCs directly following therapy (Fig. 5*B*). Also, the invasiveness of the recurrent tumors is markedly increased following intervention which is not effective against CSCs (Fig. 5*C*). These findings are in line with a range of clinical observations describing increased growth speed and enhanced invasion in the relapsing malignancy that are mostly attributed to the selection of more aggressive clones by the drug (29–31). However, our data now indicate that these observations could be partially explained by the failure of conventional therapies to eradicate the CSC compartment and the subsequent relapse dynamics in CSC-driven tumors. Evaluation of evolutionary dynamics during relapse after both types of intervention revealed significant differences as well. Following therapy which is ineffective against CSCs, relapsing tumors display a marked increase in heterogeneity, whereas therapy that does target CSCs results in a dramatic decrease of heterogeneity (Supplementary Fig. S8). This latter scenario is related to the fact that relapses are very much different compared with the primary malignancy with respect to the clonal lineages that contribute to the relapse of the tumor (Fig. 5*D*). Combined, this implicates that applying therapy that is ineffectively targeting the CSC population is not only unsuccessful in curing the patient but also promotes malignant features including rapid expansion, increased invasion, and stimulates heterogeneity directly after therapy.

## Discussion

We have applied a computational tumor growth model to investigate the effects of hierarchical organization on a range of areas in tumor biology. The obtained results provide novel insights into the influence of CSC-driven tumor growth on tumor morphology and invasion. Importantly, we have been able to partially validate these findings in a biological experimental setting. We have also established a significant effect of hierarchical organized malignant clones on tumor evolution, and consequently, on tumor progression and relapse after therapy. Our results stress the need to develop therapeutic interventions that efficiently target the CSC compartment because drugs that fail to do so are not only unable to cure the patient—but even enhance the malignant properties of tumors. Therefore, we conclude that computational oncology has the potential to greatly enhance our understanding of fundamental cancer biology and improve future therapeutics.

***CSC-Driven tumor growth.*** The capacity to display infiltrative growth is a pathognomic feature of malignant cells (1). Crossing tissue boundaries is the first step in the process of metastasis and is therefore of special interest. Surprisingly, this aspect of tumor growth has rarely been investigated in mathematical models. However, recent important work of Anderson and colleagues (11) and Bearer and colleagues (32) illuminate how selective pressure, applied by the microenvironment, in combination with tumor cell heterogeneity, could result in an invasive morphology. Here, we report how, in the SCA model, invasion emerges from the hierarchical organization of malignant clones and need not be driven by external interaction with a heterogeneous microenvironment. Hence, invasive morphology is an intrinsic feature of CSC-driven malignancies and has to be considered when studying tumor invasion.

Simultaneously, high levels of clonal heterogeneity within malignancies are associated with rapid progression of the disease (33), poorer survival (34), and occurrence of therapy resistance (35). Understanding this phenomenon in more detail might improve the design of more effective treatments and chemopreventives. Our results show how CSC-driven tumor growth stimulates heterogeneity in malignancies. This is related to the reduced effective population size in these malignancies and the typical growth pattern that results in the segregation of clones by formation of small invasive lesions. These satellite structures are not in direct competition with the dominant clone, allowing suboptimal clones to expand. We speculate that interfering with these dynamics, for example by inhibiting migration, and thereby segregation, might be a potent means by which reduced heterogeneity accompanied by the slower progression of the disease and better response to therapy can be achieved either in a chemopreventive or therapeutic setting.

Additionally, our results underlie the need to develop therapeutic modalities that successfully eradicate the CSC compartment. We show how therapeutic interventions that do not target CSCs efficiently are not only ineffective as a cure, but might even contribute to an increase in malignant properties of the relapsing tumor. We find, for example, enhanced heterogeneity and invasion in the relapsing tumors that are treated with interventions that are only directed against the differentiated cells. This is not due to the selection of the most malignant clones present in the cancer tissue but are intrinsic to the dynamics of regrowth in CSC-driven malignancies.

***Experimental validation and future directions.*** The model presented provides a range of predictions and implications regarding CSC-fuelled tumor growth that can be tested and exploited to investigate the properties of hierarchical organized malignancies. Here, we report that the clonogenicity of cell lines is connected with the invasive properties of these lines *in vitro* as suggested by our model. In future research, it would be interesting to expand this finding to human tumor specimens or in established CSC lines in which the CSC fraction can be manipulated. Additionally, our model illuminates how tumor features, such as clonal heterogeneity, are related to the CSC fraction (Supplementary Fig. S7*B*). Therefore, we speculated that careful analysis of these tumor properties might lead to optimized techniques that establish the CSC fraction in malignancies without the need for transplantation studies which are currently highly disputed (36, 37).

The current version of the SCA model clearly shows the dynamics of CSC-driven tumor growth and its consequences for tumor morphology and evolution. However, further research efforts will undoubtedly lead to increased insight into the nature of the hierarchical organization of tumor cells. If so, the SCA model can be easily adapted to implement potential new information and subsequently come to even more accurate description of tumor growth. For instance, we have assumed several variables such as CSC self-renewal frequency,

mutation rate, and migration speed to be constant. However, in *in vivo* tumors, these variables might be more dynamic both throughout tumor progression and as a consequence of microenvironmental interactions. For example, CSCs have been suggested to reside in a so-called "CSC niche" that is formed by secreted factors and direct cell-cell interactions (38, 39). This niche is believed to protect CSC from differentiation and to promote CSC self-renewal and therefore introduces dynamic $P_S$ values. Moreover, physical circumstances such as oxygen concentration might have differential effects on CSCs and DCCs, and therefore, might play a role in dynamic CSC functions (40). In addition, mutation rates are potentially subject to changes during tumor development (41) and intriguingly, might even be influenced by environmental conditions, such as that reported for bacteria (42). Currently, it remains elusive as to what extent this latter phenomenon, which is referred to as "adaptive mutation," is involved in human malignancies (43). All these considerations justify further investigations, but will be dependent on thorough experimental examination of the variables involved.

Importantly, from the current formulation of the SCA model, it is indisputable that hierarchical organization of malignancies significantly contributes to the invasive morphology and increased heterogeneity of tumors and is therefore a crucial issue for better understanding tumor biology and to improve current anticancer treatments.

## Disclosure of Potential Conflicts of Interest

No potential conflicts of interest were disclosed.

## Acknowledgments

We thank M.R. Sprick, D.J. Richel, and F. de Sousa Mello for useful comments and R. Belleman and J.H. de Jong for technical assistance.

## Grant Support

Academic Medical Center (J.J.C. Verhoeff, J.P. Medema, and L. Vermeulen), ZonMW VICI program (J.P. Medema), and the Faculty of Science of the University of Amsterdam (A. Sottoriva, L. Naumov, and P.M.A. Sloot).

The costs of publication of this article were defrayed in part by the payment of page charges. This article must therefore be hereby marked *advertisement* in accordance with 18 U.S.C. Section 1734 solely to indicate this fact.

Received 6/15/09; revised 10/20/09; accepted 10/20/09; published OnlineFirst 12/29/09.

## References

1. Hanahan D, Weinberg RA. The hallmarks of cancer. Cell 2000;100:57–70.
2. Vermeulen L, Sprick MR, Kemper K, Stassi G, Medema JP. Cancer stem cells—old concepts, new insights. Cell Death Differ 2008;15:947–58.
3. Reya T, Morrison SJ, Clarke MF, Weissman IL. Stem cells, cancer, and cancer stem cells. Nature 2001;414:105–11.
4. Sloot PMA, Hoekstra AG. Modeling dynamic systems with cellular automata. In: Fishwick PA, editor. Handbook of dynamic system modeling. Chapman & Hall/CRC; 2007, p. 1–20.
5. Nowell PC. The clonal evolution of tumor cell populations. Science 1976;194:23–8.
6. Vermeulen L, Todaro M, de Sousa Mello F, et al. Single-cell cloning of colon cancer stem cells reveals a multi-lineage differentiation capacity. Proc Natl Acad Sci U S A 2008;105:13427–32.
7. Singh SK, Hawkins C, Clarke ID, et al. Identification of human brain tumour initiating cells. Nature 2004;432:396–401.
8. Clarke MF, Dick JE, Dirks PB, et al. Cancer stem cells—perspectives on current status and future directions: AACR Workshop on Cancer Stem Cells. Cancer Res 2006;66:9339–44.
9. Araujo RP, McElwain DL. A history of the study of solid tumour growth: the contribution of mathematical modelling. Bull Math Biol 2004;66:1039–91.
10. Anderson AR, Quaranta V. Integrative mathematical oncology. Nat Rev Cancer 2008;8:227–34.
11. Anderson AR, Weaver AM, Cummings PT, Quaranta V. Tumor morphology and phenotypic evolution driven by selective pressure from the microenvironment. Cell 2006;127:905–15.
12. Sutherland RM. Cell and environment interactions in tumor microregions: the multicell spheroid model. Science 1988;240:177–84.
13. Folkman J, Hochberg M. Self-regulation of growth in three dimensions. J Exp Med 1973;138:745–53.
14. Vaupel P, Hockel M. Blood supply, oxygenation status and metabolic micromilieu of breast cancers: characterization and therapeutic relevance. Int J Oncol 2000;17:869–79.
15. Zaman MH, Trapani LM, Sieminski AL, et al. Migration of tumor cells in 3D matrices is governed by matrix stiffness along with cell-matrix adhesion and proteolysis. Proc Natl Acad Sci U S A 2006;103:10889–94.
16. Anderson AR. A hybrid mathematical model of solid tumour invasion: the importance of cell adhesion. Math Med Biol 2005;22:163–86.
17. Brabletz T, Jung A, Spaderna S, Hlubek F, Kirchner T. Opinion: migrating cancer stem cells—an integrated concept of malignant tumour progression. Nat Rev Cancer 2005;5:744–9.
18. Hermann PC, Huber SL, Herrler T, et al. Distinct populations of cancer stem cells determine tumor growth and metastatic activity in human pancreatic cancer. Cell Stem Cell 2007;1:313–23.
19. Laird DJ, von Andrian UH, Wagers AJ. Stem cell trafficking in tissue development, growth, and disease. Cell 2008;132:612–30.
20. Sheridan C, Kishimoto H, Fuchs RK, et al. CD44+/CD24– breast cancer cells exhibit enhanced invasive properties: an early step necessary for metastasis. Breast Cancer Res 2006;8:R59.
21. Balic M, Lin H, Young L, et al. Most early disseminated cancer cells detected in bone marrow of breast cancer patients have a putative breast cancer stem cell phenotype. Clin Cancer Res 2006;12:5615–21.
22. Dormann S, Deutsch A. Modeling of self-organized avascular tumor growth with a hybrid cellular automaton. In Silico Biol 2002;2:393–406.
23. Jiang Y, Pjesivac-Grbovic J, Cantrell C, Freyer JP. A multiscale model for avascular tumor growth. Biophys J 2005;89:3884–94.
24. Enderling H, Hlatky L, Hahnfeldt P. Migration rules: tumours are conglomerates of self-metastases. Br J Cancer 2009;100:1917–25.
25. Merlo LM, Pepper JW, Reid BJ, Maley CC. Cancer as an evolutionary and ecological process. Nat Rev Cancer 2006;6:924–35.
26. Mayr E. Change of genetic environment and evolution. In: Huxley J, Hardy AC, Ford EB, editors. Evolution as a process. Princeton: Princeton University Press; 1954, p. 157–80.
27. Jordan CT, Guzman ML, Noble M. Cancer stem cells. N Engl J Med 2006;355:1253–61.
28. Rich JN. Cancer stem cells in radiation resistance. Cancer Res 2007;67:8980–4.

29. Huff CA, Matsui W, Smith BD, Jones RJ. The paradox of response and survival in cancer therapeutics. Blood 2006;107:431–4.
30. Spiegl-Kreinecker S, Pirker C, Marosi C, et al. Dynamics of chemosensitivity and chromosomal instability in recurrent glioblastoma. Br J Cancer 2007;96:960–9.
31. El Sharouni SY, Kal HB, Battermann JJ. Accelerated regrowth of non-small-cell lung tumours after induction chemotherapy. Br J Cancer 2003;89:2184–9.
32. Bearer EL, Lowengrub JS, Frieboes HB, et al. Multiparameter computational modeling of tumor invasion. Cancer Res 2009;69: 4493–501.
33. Maley CC, Galipeau PC, Finley JC, et al. Genetic clonal diversity predicts progression to esophageal adenocarcinoma. Nat Genet 2006; 38:468–73.
34. Flyger HL, Larsen JK, Nielsen HJ, Christensen IJ. DNA ploidy in colorectal cancer, heterogeneity within and between tumors and relation to survival. Cytometry 1999;38:293–300.
35. Iwasa Y, Nowak MA, Michor F. Evolution of resistance during clonal expansion. Genetics 2006;172:2557–66.
36. Hill RP. Identifying cancer stem cells in solid tumors: case not proven [discussion 0]. Cancer Res 2006;66:1891–5.
37. Quintana E, Shackleton M, Sabel MS, Fullen DR, Johnson TM, Morrison SJ. Efficient tumour formation by single human melanoma cells. Nature 2008;456:593–8.
38. Gilbertson RJ, Rich JN. Making a tumour's bed: glioblastoma stem cells and the vascular niche. Nat Rev Cancer 2007;7:733–6.
39. Borovski T, Verhoeff JJ, ten Cate R, et al. Tumor microvasculature supports proliferation and expansion of glioma-propagating cells. Int J Cancer 2009;125:1222–30.
40. Li Z, Bao S, Wu Q, et al. Hypoxia-inducible factors regulate tumorigenic capacity of glioma stem cells. Cancer Cell 2009;15:501–13.
41. Bielas JH, Loeb KR, Rubin BP, True LD, Loeb LA. Human cancers express a mutator phenotype. Proc Natl Acad Sci U S A 2006;103: 18238–42.
42. Hastings PJ, Bull HJ, Klump JR, Rosenberg SM. Adaptive amplification: an inducible chromosomal instability mechanism. Cell 2000; 103:723–31.
43. Rosenberg SM. Evolving responsively: adaptive mutation. Nat Rev Genet 2001;2:504–15.
44. Tomita K, Plager JE. *In vivo* cell cycle synchronization of the murine sarcoma 180 tumor following alternating periods of hydroxyurea blockade and release. Cancer Res 1979;39:4407–11.
45. Sherwood L. Human physiology: from cells to systems. Belmont: Wadsworth Publishing Company; 1997.
46. Casciari JJ, Sotirchos SV, Sutherland RM. Variations in tumor cell growth rates and metabolism with oxygen concentration, glucose concentration, and extracellular pH. J Cell Physiol 1992;151:386–94.
47. Freyer JP, Tustanoff E, Franko AJ, Sutherland RM. *In situ* oxygen consumption rates of cells in V-79 multicellular spheroids during growth. J Cell Physiol 1984;118:53–61.
48. Bray D. Cell movements. New York: Garland Pub.; 1992.